

The Neutrino Mass Bound from Leptogenesis Revisited

Björn Garbrecht^a and Edward Wang^b

*Physik-Department T70, Technische Universität München,
James-Franck-Straße, 85748 Garching, Germany*

Recent years have seen a great improvement in the computation of CP -conserving and CP -violating equilibration rates for leptogenesis. These are relevant for the relativistic regime of the sterile Majorana fermions and the dynamics of the Standard Model particles acting as spectator processes. In order to probe the regime of large ($\mathcal{O}(10^2)$) washout parameters, we add $\Delta L = 2$ washout processes, which we derive in the CTP-formalism. To demonstrate their significance, we apply state-of-the-art computational techniques to a simple yet well-motivated phenomenological scenario: unflavored leptogenesis in a hierarchical type-I seesaw model. We then perform a parameter scan of the final baryon asymmetry and find a constraint $m_{\text{lightest}} \lesssim 0.15$ eV on the absolute neutrino mass scale, which is slightly less stringent than previously reported bounds obtained without the aforementioned improvements. The relaxation of the bounds is mainly due to partially equilibrated spectator fields, which protect part of the asymmetry from washout and lead to larger final asymmetries. While this might seem like a minor correction, the actual dynamics of the fields is substantially altered by these effects. Even though we focused on a particularly simple scenario for leptogenesis, the methods employed here can and should be extended to other models, thus giving us a more accurate picture of the different leptogenesis scenarios.

I. Introduction

Leptogenesis is a framework that connects two of the long-standing problems of the Standard Model: the origin of neutrino masses and of the baryon asymmetry of the Universe (BAU). If neutrino masses are produced through the coupling to a Majorana fermion, its out-of-equilibrium decay could produce a lepton asymmetry in the early Universe, which would then be converted into a baryon asymmetry via sphaleron processes. One of the first and most compelling proposals to explain the neutrino masses is the seesaw mechanism, in which active neutrinos couple to heavy Majorana fermions via the Higgs boson. One can then find that large Majorana masses naturally explain the smallness of neutrino masses.

The simplest scenario of leptogenesis in the seesaw model is the case of strongly hierarchical Majorana fermions $M_2, M_3 \gg M_1$ without flavour effects. In this setup, an upper bound on the neutrino masses, parametrized by the lightest neutrino mass $m_{\text{lightest}} \lesssim 0.12$ eV was found [1–3]. This bound is in agreement with cosmological bounds on neutrino masses, with the constraint $\sum m_\nu < 0.12$ eV (95% C.L.) from Planck [4], corresponding to $m_{\text{lightest}} < 0.03(0.016)$ eV in normal (inverted) hierarchy, while DESI [5] further tightened this constraint to $\sum m_\nu < 0.072$ eV (95% C.L.), corresponding to $m_{\text{lightest}} < 0.0086$ eV in normal hierarchy and below the threshold for inverted hierarchy. However, given the many tensions in cosmological data and between cosmological and terrestrial constraints, the robustness of these bounds is yet to be confirmed [6–10]. In view of this, the best model-independent constraint is given by the KATRIN experiment, which placed an upper bound on the effective electron antineutrino mass $m_{\text{lightest}} \approx m_e = \sqrt{\sum_i |U_{ei}|^2 m_i^2} < 0.8$ eV (90% C.L.) [11]. Additionally, in the absence of cancellations due to new physics effects, KamLAND-Zen also places a constraint $m_{\text{lightest}} < 0.18 - 0.48$ eV (90% C.L.) from neutrinoless double beta decay assuming Majorana masses [12]. While KamLAND-Zen has since obtained a stronger constraint on the effective Majorana mass $\langle m_{\beta\beta} \rangle$ [13], its translation into a bound on m_{lightest} depends on the mass hierarchy. Given recent improvements on the computation of the fluid equations for leptogenesis [14], it is interesting to investigate how these affect the predictions of leptogenesis for different neutrino mass scales.

As far as the dynamics of leptogenesis is concerned, a value of $m_{\text{lightest}} \approx 0.14$ eV that we find in our analysis pushes $M_1 \gtrsim 5 \times 10^{12}$ eV. At the corresponding temperatures, tau-Yukawa couplings are out of equilibrium so that leptogenesis is in the unflavoured regime. In view of our interest in the upper bound on m_{lightest} , for definiteness and for the sake of comparison with earlier papers, we therefore do not include flavour effects in the present analysis, even though they will become relevant on the lower side of the values of M_1 that appear allowed by the unflavoured calculation.

^a garbrecht@tum.de

^b edward.wang@tum.de

The improvements in Ref. [14] mainly focus on two aspects: the careful computation of the rates in the relativistic regime of the lightest Majorana fermion and the inclusion of spectator effects. In the relativistic regime, there are thermal contributions to the rates and to the decay asymmetry that become relevant, and, in addition to this, the interactions are sensitive to the helicity of the Majorana fermions. It is therefore necessary to track the evolution of the different helicity states separately. In the weak washout regime, a significant fraction of this early asymmetry survives at late times, while in the strong washout regime part of the asymmetry gets protected by spectator fields. The precise computation of these early processes is therefore of great relevance for an accurate estimate of the lepton asymmetry at late times.

In Ref. [14], these methods were applied to a simplified version of the seesaw model to demonstrate the impact of these new effects. In the present work we will apply them to a seesaw model relevant for neutrino mass generation, and investigate the interplay between the parameters for neutrino masses and for leptogenesis. In addition to this, we include a treatment of $\Delta L = 2$ processes within the CTP-framework, which was absent in previous works that have introduced an improved treatment of Majorana fermions in the relativistic regimes as well as the dynamics of spectator effects. Subsequent to the analysis of neutrino mass bounds in unflavoured leptogenesis [1–3], it has been shown that the aforementioned flavour effects allow one to lower the scale of leptogenesis and to relax many constraints (for a review, see Ref. [15]). Further, if the reheat temperature is high enough, also the lepton asymmetry from the out-of-equilibrium dynamics of the next-to-lightest sterile Majorana fermion may survive washout from the lightest one and thus directly contribute to the outcome of leptogenesis [16]. Yet, the simple unflavoured scenario remains a viable possibility within the seesaw parameter space, and it is illustrative of the relevance of these new methods for phenomenological models of leptogenesis. The applicability of these methods is, however, not restricted to this simplified case, but rather general.

The outline of the article is as follows: in Section II we present the realization of the seesaw model we will employ, and discuss properties of the neutrino mass mechanism as well as of the decay asymmetry of N_1 in vacuum within this model. In Section III we discuss the fluid equations with the effects described above. In Section IV we present our treatment of the $\Delta L = 2$ processes and in Section V we show the results from our numerical scan of the asymmetry for different choices of the parameters. We conclude with Section VI.

II. The Model

The model we consider is the usual type-I seesaw model with three sterile Majorana neutrinos, given by

$$\mathcal{L} = \mathcal{L}_{SM} + \frac{1}{2} \bar{N}_i i\bar{\phi} N_i - \frac{1}{2} M_i \bar{N}_i N_i - h_{ij} \bar{\ell}_i \tilde{\phi} N_j - h_{ij}^* \bar{N}_j \tilde{\phi}^* \ell_i, \quad (1)$$

where $\tilde{\phi} = i\sigma_2 \phi^*$ is the Higgs doublet conjugated with respect to weak hypercharge and isospin. We further assume strongly hierarchical masses $M_1 \ll M_2 \ll M_3$. After electroweak symmetry breaking, the Higgs field acquires a vacuum expectation value $\sqrt{2} \langle \phi_0 \rangle = v = 246 \text{ GeV}$, producing the Dirac neutrino mass matrix $m_D = hv/\sqrt{2}$. Upon diagonalization of the mass matrix we find the light neutrino mass matrix

$$m_\nu = m_D M^{-1} m_D^T, \quad (2)$$

with real and positive eigenvalues m_1, m_2 and m_3 . In the neutrino mass eigenbasis, one can show that the vacuum CP -asymmetry of the N_1 decay is given by [17–19]

$$\epsilon_0 = \frac{3}{4\pi} \frac{M_1}{v^2} \sum_{i \neq 1} \frac{\Delta m_{i1}^2}{m_i} \frac{\text{Im}(h_{i1}^2)}{(h^\dagger h)_{11}}, \quad (3)$$

where $\Delta m_{i1}^2 = m_i^2 - m_1^2$. As shown in Ref. [20], with the approximation $m_2 \sim m_1$, we can express the maximal asymmetry as

$$\epsilon_{\max} = \max_y \frac{3}{16\pi} \frac{M_1}{v^2} \frac{m_3^2 - m_1^2}{\tilde{m}_1} \sinh 2y \sqrt{1 - \left(\frac{2\tilde{m}_1 - (m_1 + m_3)\cosh 2y}{m_3 - m_1} \right)^2}. \quad (4)$$

It is useful to introduce the washout parameter [21, 22]

$$K = \frac{\Gamma_D(z = \infty)}{H(z = 1)}, \quad (5)$$

where $\Gamma_D(z = \infty) = (h^\dagger h)_{11} M_1 / (8\pi)$ is the decay width of N_1 , as well as the effective neutrino mass [23]

$$\tilde{m}_1 = \frac{(m_D^\dagger m_D)_{11}}{M_1}, \quad (6)$$

which are related as

$$K = \frac{\tilde{m}_1}{m_*}, \quad (7)$$

where

$$m_* = \frac{16\pi v^2}{m_{Pl}} \sqrt{\frac{g_* \pi^3}{45}}, \quad (8)$$

is the equilibrium neutrino mass [24, 25], with $m_{Pl} = 1.22 \times 10^{19}$ GeV the Planck mass and $g_* = 106.75$ the number of relativistic degrees of freedom. The structure of the neutrino mass matrix yields the constraint $\tilde{m}_1 \geq m_{\text{lightest}}$.

Following the approach from Ref. [26], we describe the early Universe by a spatially flat Friedman-Lemaître-Robertson-Walker (FLRW) metric. We can then shift our description into comoving coordinates, with comoving quantities defined as $\vec{k} = a(t)\vec{k}_{\text{phys}}$, $T = a(t)T_{\text{phys}}$ and $s = a(t)^3 s_{\text{phys}}$, where $a(t)$ is the scale factor of the FLRW metric. Here, T is the temperature, \vec{k} momentum and s the entropy density; and we have indicated the physical parameters with a subscript ‘phys’. Introducing the conformal time η , related to t by $dt = ad\eta$, the scale factor in the radiation-dominated Universe is given by $a = a_R\eta$. We choose

$$a_R = T = \frac{m_{Pl}}{2} \sqrt{\frac{45}{g_* \pi^3}}. \quad (9)$$

In this way, the effect of the expansion of the Universe is described by masses that scale with a . We further introduce the dimensionless time variable $z = M_1/T_{\text{phys}}$. With this we can write the washout parameter as

$$K = \frac{g_w a_R (h^\dagger h)_{11}}{16\pi M_1}. \quad (10)$$

One commonly distinguishes the scenarios of strong and weak washout, characterized by the conditions $K > 1$ and $K < 1$ respectively.

Additionally, we approximate the Standard Model particles as being in kinetic equilibrium, so that the charge asymmetries can be parametrized by their respective chemical potentials. For small chemical potentials and relativistic particles, we have

$$\mu_X \approx \frac{3g_s s}{T^2} Y_X, \quad (11)$$

with $g_s = 2$ for fermions and $g_s = 1$ for scalars.

III. Fluid Equations for Leptogenesis

In our description of leptogenesis we employ momentum-averaged fluid equations, which in general leads to an order one uncertainty in the final asymmetry [27, 28]; however, this approximation works well in the strong washout regime due to the nonrelativistic kinematics of the sterile Majorana fermions [29, 30]. Throughout this work we will use the Schwinger-Keldysh Closed-Time-Path (CTP) formalism [31, 32] applied to nonequilibrium quantum-field theory [33]. This allows for a self-consistent treatment of the rates from first principles.

Leptogenesis can be described by a set of coupled kinetic equations, which, in its simplest scenario, is given by

$$\frac{d}{dz} Y_{N1} = -\Gamma_D (Y_{N1} - Y_{N1}^{\text{eq}}), \quad (12a)$$

$$\frac{d}{dz} Y_\ell = -\epsilon_0 \Gamma_D (Y_{N1} - Y_{N1}^{\text{eq}}) - \Gamma_W Y_\ell, \quad (12b)$$

where we define the particle yields

$$Y_X = \frac{1}{s}(n_X^+ - n_X^-), \quad (13)$$

with $n_X^{+,-}$ the particle and antiparticle number densities for species X . For Majorana fermions, for which the distinction between particle and antiparticle does not apply, we instead use

$$Y_N = \frac{1}{s}n_N. \quad (14)$$

In Eq. (12b), Γ_W are washout rates, which comprise inverse decays and lepton number violating scatterings.

As discussed in Ref. [14], the description through Eqs. (12) are incomplete for a number of reasons. The first is the handling of the Majorana particles. The decay rate Γ_D is the vacuum decay rate of Majorana particles at rest. As the authors of that paper showed through direct numerical comparison, this rate is sufficiently accurate for $z \gtrsim 10$. For $z \lesssim 10$, however, one needs to take into account the dilation of the decay rate, and for $z \lesssim 1$ thermal effects also become relevant. The second issue is that Eqs. (12) make no distinction between the helicity states of the Majorana fermion, which is relevant for relativistic particles. Both of these issues have been addressed in Ref. [14] in the derivation of the rates in the CTP formalism.

We denote by ℓ_{\parallel} the linear combination of leptons that couple to N_1 , by B baryon and L lepton number. Noting that in the temperature range of interest above 10^{13} GeV lepton flavour is conserved and assuming the particles N_1 are the only source of asymmetry, we can set $Y_{\Delta_{\parallel}} = Y_{B/3} - 2Y_{\ell_{\parallel}} = Y_{B-L}$. Further, we define the even and odd combinations of helicity

$$Y_{N_{\text{even/odd}}} = \frac{1}{s}(n_{N+} \pm n_{N-}). \quad (15)$$

In terms of these quantities, one arrives at the relativistic fluid equations

$$\frac{d}{dz}Y_{N_1\text{even}} = -\Gamma \cdot (Y_{N_1\text{even}} - Y_{N_1\text{eq}}), \quad (16a)$$

$$\frac{d}{dz}Y_{N_1\text{odd}} = -\Gamma \cdot Y_{N_1\text{odd}} - \eta_{N_1}\tilde{\Gamma} \cdot (Y_{\ell_{\parallel}} + \frac{1}{2}Y_{\phi}), \quad (16b)$$

$$\frac{d}{dz}Y_{\Delta_{\parallel}} = \tilde{\Gamma} \cdot Y_{N_1\text{odd}} - \epsilon_{\text{eff}}\Gamma \cdot (Y_{N_1\text{even}} - Y_{N_1\text{eq}}) + \eta_{N_1}\Gamma \cdot (Y_{\ell_{\parallel}} + \frac{1}{2}Y_{\phi}). \quad (16c)$$

Here we have introduced the rates

$$\Gamma = K\frac{1}{2}(\gamma_{\text{LNC}} + \gamma_{\text{LNV}}), \quad \tilde{\Gamma} = K\frac{1}{2}(\gamma_{\text{LNC}} - \gamma_{\text{LNV}}) \quad (17)$$

and the effective CP -violating parameter at finite temperature

$$\epsilon_{\text{eff}} = \epsilon_0 \frac{\mathcal{K}(z)}{\mathcal{I}(z)} \frac{2\gamma_{\text{LNC}} \cdot \gamma_{\text{LNV}}}{z^2(\gamma_{\text{LNC}} + \gamma_{\text{LNV}})}, \quad (18)$$

which depend on the lepton-number conserving and violating rates γ_{LNC} and γ_{LNV} respectively, and with

$$\mathcal{I}(z) = \int_z^{\infty} dy \frac{y\sqrt{y^2 - z^2}}{e^y + 1} = z^2 \sum_{n=1}^{\infty} \frac{(-1)^{n+1}}{n} K_2(nz) \approx z^2 K_2(z), \quad (19)$$

$$\mathcal{J}(z) = \int_z^{\infty} dy \frac{y\sqrt{y^2 - z^2}e^y}{(e^y + 1)^2} = z^2 \sum_{n=1}^{\infty} (-1)^{n-1} K_2(nz) \approx z^2 K_2(z), \quad (20)$$

$$\mathcal{K}(z) = \int_z^{\infty} dy \frac{y^2\sqrt{y^2 - z^2}}{e^y + 1} = \sum_{n=1}^{\infty} (-1)^{n+1} \left(\frac{z^3}{n} K_1(nz) + \frac{3z^2}{n^2} K_2(nz) \right) \approx z^3 K_1(z) + 3z^2 K_2(z). \quad (21)$$

In terms of these we can also write

$$Y_{N_1\text{eq}}(z) = \frac{T^3}{s\pi^2} \mathcal{I}(z), \quad \eta_{N_1}(z) = \frac{6}{\pi^2} \mathcal{J}(z). \quad (22)$$

In the case of fully equilibrated spectators, that is strong and weak sphalerons as well as top and bottom-Yukawa interactions in the temperature range of interest, one obtains the relations

$$Y_{\ell_{\parallel}} = -\frac{13}{30}Y_{\Delta_{\parallel}}, \quad Y_{\phi} = -\frac{1}{5}Y_{\Delta_{\parallel}}. \quad (23)$$

We take the numerical data points for γ_{LNC} and γ_{LNV} obtained in Ref. [14] and interpolate between them to compute our rates. Note that for $z \rightarrow 0$, γ_{LNV} vanishes because the lepton-number violation through the Majorana mass M_1 becomes irrelevant at high temperatures. For $z \gtrsim 1$, one recovers $\gamma_{\text{LNC}} \approx \gamma_{\text{LNV}}$, indicating that a $1 \leftrightarrow 2$ process between N_1 , ℓ and ϕ violates lepton number at a coin-toss chance. As for the parameter ϵ_{eff} , sizeable early asymmetries can be produced at small z in spite of the suppression of γ_{LNV} because it is compensated by a large deviation of N_1 from equilibrium—an effect more sizeable for vanishing than for thermal initial conditions of N_1 .

While these relativistic effects are irrelevant if the early asymmetries are destroyed by strong washout, they can have a sizeable effect in the weak washout regime or in the presence of partially equilibrated spectator fields which protect some of the asymmetry from washout. To describe the spectator fields we introduce the quark yields Y_{Q_i} for the left-handed doublets, and $Y_{u_i}, Y_{d_i}, Y_t, Y_b, i = 1, 2$ for the right-handed singlets, as well as the lepton fields not coupling to N_1 directly $Y_{\ell_{\perp 1}}, Y_{\ell_{\perp 2}}$. Since at high temperatures the lepton and the first and second quark generation Yukawa couplings are negligible, we can set $Y_{u_i} = Y_{d_i} = Y_d$, $Y_{Q_1} = Y_{Q_2} = Y_Q$ and $Y_{\ell_{\perp 1}} = Y_{\ell_{\perp 2}} = Y_{\ell_{\perp}}$. At $T \sim 10^{13}$ GeV, the relevant partially equilibrated interactions are bottom-Yukawa and weak sphaleron interactions. Defining $Y_{\Delta_{\text{down}}} = Y_b - Y_d$, the full system of Boltzmann equations is [34]

$$\frac{d}{dz}Y_{N_1\text{even}} = -\Gamma \cdot (Y_{N_1\text{even}} - Y_{N_1\text{eq}}), \quad (24a)$$

$$\frac{d}{dz}Y_{N_1\text{odd}} = -\Gamma \cdot Y_{N_1\text{odd}} - \eta_{N_1}\tilde{\Gamma} \cdot (Y_{\ell_{\parallel}} + \frac{1}{2}Y_{\phi}), \quad (24b)$$

$$\frac{d}{dz}Y_{\Delta_{\parallel}} = \tilde{\Gamma} \cdot Y_{N_1\text{odd}} - \epsilon_{\text{eff}}\Gamma \cdot (Y_{N_1\text{even}} - Y_{N_1\text{eq}}) + \eta_{N_1}\Gamma \cdot (Y_{\ell_{\parallel}} + \frac{1}{2}Y_{\phi}), \quad (24c)$$

$$\frac{d}{dz}Y_{\Delta_{\text{down}}} = -\Gamma_{\text{down}} \cdot (Y_b - Y_{Q_3} + \frac{1}{2}Y_{\phi}), \quad (24d)$$

$$\frac{d}{dz}Y_{\ell_{\perp}} = -\Gamma_{\text{ws}} \cdot (9Y_{Q_3} + 18Y_Q + 3Y_{\ell_{\parallel}} + 6Y_{\ell_{\perp}}), \quad (24e)$$

with the equilibration rates [34–36]

$$\Gamma_{\text{down}} \approx 1.0 \times 10^{-2} \frac{h_b^2 T}{M_1}, \quad \Gamma_{\text{ws}} \approx (8.24 \pm 0.10) \left(\log \left(\frac{m_D}{g_2^2 T} \right) + 3.041 \right) \frac{g_2^2 T^3}{2m_D^2 M_1} \alpha_2^5, \quad (25)$$

with h_b the bottom-Yukawa coupling, $\alpha_2 = g_2^2/4\pi$ the $SU(2)_L$ electroweak coupling strength and $m_D^2 \approx \frac{11}{6}g_2^2 T^2$ the thermal mass of the $SU(2)_L$ gauge bosons.

In addition to this, we need to relate the yields $Y_{\ell_{\parallel}}, Y_{Q_3}, Y_b, Y_Q, Y_{\phi}$ to $Y_{\Delta_{\parallel}}, Y_{\ell_{\perp}}, Y_{\Delta_{\text{down}}}$ in order to obtain a closed system of equations. From the constraints on the chemical potentials following from the top-quark Yukawa-couplings and strong sphalerons being in equilibrium, we find the relations

$$\begin{pmatrix} Y_{\ell_{\parallel}} \\ Y_{Q_3} \\ Y_b \\ Y_Q \\ Y_{\phi} \end{pmatrix} = \begin{pmatrix} -\frac{1}{2} & 1 & 0 \\ \frac{1}{23} & \frac{1}{2} & -\frac{10}{23} \\ \frac{1}{46} & \frac{1}{2} & \frac{18}{23} \\ -\frac{1}{46} & \frac{1}{2} & \frac{5}{23} \\ -\frac{7}{23} & 0 & \frac{24}{23} \end{pmatrix} \begin{pmatrix} Y_{\Delta_{\parallel}} \\ Y_{\ell_{\perp}} \\ Y_{\Delta_{\text{down}}} \end{pmatrix}. \quad (26)$$

In the present scenario, the early asymmetries in Y_{ϕ} are transferred through the B and L -conserving bottom-Yukawa couplings to $Y_{\Delta_{\text{down}}}$, as described by Eq. (24d). There, the asymmetry is effectively hidden from washout through N_1 , as long as the bottom-Yukawa coupling doesn't fully equilibrate. The down-quark asymmetry maintains an asymmetry in ϕ , which in turn creates a bias in ℓ_{\parallel} that is not fully erased as lepton-number violation through N_1 freezes out. This way, an early asymmetry in ϕ , which is neither baryonic nor leptonic, turns into a lepton asymmetry during the freeze-out of N_1 .

IV. $\Delta L = 2$ Processes

In Ref. [14], only the on-shell part of the N_1 propagator was considered, due to the smallness of the propagator width. In doing so, however, one neglects $\Delta L = 2$ contributions to the washout, which limit the lepton asymmetry for large Yukawa couplings and M_1 and are therefore paramount for the determination of the bound on m_{lightest} . In this section, we derive the $\Delta L = 2$ contribution to the washout by adding a purely off-shell part to the N_1 spectral self-energy. This off-shell part is due to loop insertions to the propagator, where the particles running in the loop are on-shell, even if the propagator itself is not. When inserting these terms into the collision term, we find that this corresponds to $\Delta L = 2$ scattering processes. In this way, we are able to determine these rates in an entirely consistent way within the CTP formalism.

One crucial difference between our result and the one from Ref. [37] is that the authors of that paper considered a washout rate averaged over all lepton flavours. When doing so and adding the interactions with all heavy Majorana fermions, a cancellation of terms similar to the one in the neutrino mass matrix occurs, such that the final rate does not depend on the specific form of the Yukawa matrix or the washout parameter K but only on the values of the neutrino masses. We improve on this approach, taking into account that the N_1 decays don't produce all lepton flavours equally, but only a specific linear combination of flavours. The interactions of ℓ_{\parallel} with the heavier Majorana fermions heavily depend on the form of the Yukawa matrix, and so the cancellation they reported doesn't occur in this case. Since we expect these interactions to be subdominant with respect to the interactions with N_1 due to their large masses, we only keep the latter ones. Even though we are considering less interaction terms than the previous analysis, for large K , the washout rates we find are larger than previously found. The reason for this is that, in the flavour-averaged case, large K terms are always cancelled by the N_2 and N_3 interaction terms. In our case, we know that this cancellation is not exact in general and so we expect a large washout rate to remain even if we were to include interactions with N_2 and N_3 in our analysis.

At a methodical level, the leading order evaluation of the CP asymmetry in the CTP formalism readily yields Boltzmann equations that predict no CP asymmetry in thermal equilibrium. We therefore need to include self-energy corrections in the spectral propagator of the Majorana neutrino to capture off-shell effects, as we shall do in the following. For comparison, in conventional setups where S-matrix elements are substituted into Boltzmann equations, the evaluation based on $1 \leftrightarrow 2$ processes and their inverse only misses leading order contributions that guarantee CP -symmetric equilibrium conditions. The missing contributions are then attributed to $2 \leftrightarrow 2$ processes, where overcounting of reactions mediated by on-shell Majorana neutrinos is dealt with by the subtraction of real intermediate states. This approach has been worked out in Ref. [38] for general scenarios of baryogenesis from out-of-equilibrium decays. It then has been applied to leptogenesis in Ref. [19], and further detailed discussion can be found in Refs. [3, 24, 37].

Similarly to the case of Standard Model leptons, the N propagator in kinetic equilibrium can be written as

$$iS_N^<(k) = -2S_N^A f_N(k), \quad iS_N^>(k) = 2S_N^A(1 - f_N(k)). \quad (27)$$

The spectral propagator for a massive fermion, when summing up the self energies, is given by

$$S_{N_1}^A(k) = \left[(\not{k} + M_1 - \Sigma_N^H(k)) \cdot \frac{\Gamma_N}{\Omega_N^2 + \Gamma_N^2} - \Sigma_N^A(k) \frac{\Omega_N}{\Omega_N^2 + \Gamma_N^2} \right], \quad (28)$$

with

$$\Gamma_N(k) = 2(k_\mu - \Sigma_{N,\mu}^H) \cdot \Sigma_N^{A,\mu}, \quad \Omega_N(k) = (k_\mu - \Sigma_{N,\mu}^H)^2 - M_1^2 - (\Sigma_{N,\mu}^A)^2. \quad (29)$$

As a subtlety, note that when ϕ and ℓ are in equilibrium, then strictly speaking only the Fermi-Dirac part of the distribution f_N in Eq. (27) goes with the finite width form of the spectral function from Eq. (28), while the out-of-equilibrium remainder should go with a sharply peaked on-shell δ -distribution. However, we may still effectively use the form as in Eq. (27) because the δ -distribution is shifted to a finite-width form when all gradients incurred as N_1 relaxes toward equilibrium are properly taken into account [39]. The N_1 self-energy can be decomposed as

$$i\Sigma_{N_1}^{>,<}(k) = g_w(h^\dagger h)_{11}(P_L \gamma_\mu i\hat{\Sigma}_{N_1,L}^{\mu>,<}(k) + P_R \gamma_\mu i\hat{\Sigma}_{N_1,R}^{\mu>,<}(k)), \quad (30)$$

with

$$i\hat{\Sigma}_{N_1,L}^{\mu>,<}(k) = \frac{1}{2} \int \frac{d^4 p}{(2\pi)^4} \text{tr}[\gamma^\mu P_L iS_{\ell_\parallel}^{>,<}(p) P_R] i\Delta_\phi^{>,<}(k-p), \quad (31)$$

$$i\hat{\Sigma}_{N_1,R}^{\mu>,<}(k) = \frac{1}{2} \int \frac{d^4 p}{(2\pi)^4} \text{tr}[\gamma^\mu P_R C(iS_{\ell_\parallel}^{<,>}(-p))^T C^\dagger P_L] i\Delta_\phi^{<,>}(p-k). \quad (32)$$

In kinetic equilibrium, they satisfy the generalized Kubo–Martin–Schwinger (KMS) relations

$$\hat{\Sigma}_{N_1,L/R}^>(k) = -e^{(k_0 \mp \mu_\ell \mp \mu_\phi)/T} \hat{\Sigma}_{N_1,L/R}^<(k), \quad (33)$$

and we can express the spectral self energies as

$$\hat{\Sigma}_{N_1,L/R}^{\mathcal{A}0}(k) = \frac{T^2}{16\pi|\mathbf{k}|} I_1 \left(\frac{k^0}{T}, \frac{|\mathbf{k}|}{T}, \pm \frac{\mu_\ell}{T}, \pm \frac{\mu_\phi}{T} \right), \quad (34a)$$

$$\hat{\Sigma}_{N_1,L/R}^{\mathcal{A}i}(k) = \frac{T^2}{16\pi|\mathbf{k}|} \frac{k^i}{|\mathbf{k}|} \left[\frac{k^0}{|\mathbf{k}|} I_1 \left(\frac{k^0}{T}, \frac{|\mathbf{k}|}{T}, \pm \frac{\mu_\ell}{T}, \pm \frac{\mu_\phi}{T} \right) - \frac{(k^0)^2 - \mathbf{k}^2}{2|\mathbf{k}|T} I_0 \left(\frac{k^0}{T}, \frac{|\mathbf{k}|}{T}, \pm \frac{\mu_\ell}{T}, \pm \frac{\mu_\phi}{T} \right) \right], \quad (34b)$$

with

$$I_0(y_0, y, u_1, u_2) = (2u_1 - y_0)\theta(y^2 - y_0^2) + \log \left(\frac{1 - e^{(|y_0+y|)/2 + (-1)^{\theta(-y_0-y)}u_2}}{1 - e^{(|y_0-y|)/2 + (-1)^{\theta(y-y_0)}u_2}} \right) + \log \left(\frac{1 + e^{(|y_0+y|)/2 + (-1)^{\theta(y_0+y)}u_1}}{1 + e^{(|y_0-y|)/2 + (-1)^{\theta(y-y_0)}u_1}} \right), \quad (35a)$$

$$I_1(y_0, y, u_1, u_2) = \frac{y|y_0|}{2} \theta(y_0^2 - y^2) + \frac{\pi^2 + u_1^2 - u_2^2 - \text{sign}(y_0)(|y_0| - y)(u_1 - u_2)}{2} \theta(-y_0^2 + y^2) + \frac{y_0 + y}{2} \log \left(\frac{1 + e^{-(|y_0+y|)/2 + (-1)^{\theta(-y_0-y)}u_1}}{1 - e^{-(|y_0-y|)/2 + (-1)^{\theta(y-y_0)}u_2}} \right) - \frac{y_0 - y}{2} \log \left(\frac{1 + e^{-|y_0-y|/2 + (-1)^{\theta(y-y_0)}u_1}}{1 - e^{-|y_0+y|/2 + (-1)^{\theta(-y_0-y)}u_2}} \right) + \text{Re} \left[\text{Li}_2 \left(-e^{-(y_0-y)/2 + \text{sign}(y_0)u_1} \right) - \text{Li}_2 \left(e^{-(y_0-y)/2 + \text{sign}(y_0)u_2} \right) - \text{Li}_2 \left(-e^{-(y_0+y)/2 + \text{sign}(y_0)u_1} \right) + \text{Li}_2 \left(e^{-(y_0+y)/2 + \text{sign}(y_0)u_2} \right) \right], \quad (35b)$$

for massless particles running in the loop. This generalizes the results from Refs. [35, 40, 41] for particles with chemical potentials in the loop and reduces to the previously known results in the case of vanishing chemical potentials.

As in Ref. [14], the collision term for charged leptons without the CP -violating source term is given by

$$g_w \frac{d}{dz} Y_{\ell_\parallel} = \frac{1}{\tilde{M}_1 s} \int \frac{d^4 k}{(2\pi)^4} \text{tr}[iS_{N_1}^>(k) P_L i\Sigma_{N_1}^<(k) - iS_{N_1}^<(k) P_L i\Sigma_{N_1}^>(k)]. \quad (36)$$

Since in the relevant parameter region the Yukawa couplings are comparatively small, we can neglect the width of N_1 while retaining the off-shell part of the propagator. We can then write¹

$$S_{N_1}^{\mathcal{A}}(k) \approx \pi \delta(k^2 - M_1^2) \text{sign}(k^0) (\not{k} + M_1) - \frac{\Sigma_N^{\mathcal{A}}(k)}{k^2 - M_1^2}. \quad (37)$$

Taking the off-shell part of the propagator and using the KMS relation for the self-energy, we can write

$$g_w \frac{d}{dz} Y_{\ell_\parallel} = -\frac{8g_w^2 (h^\dagger h)_{11}^2}{\tilde{M}_1 s} \int \frac{d^4 k}{(2\pi)^4} (f_F(k_0 - \mu_\ell - \mu_\phi) - f_F(k_0 + \mu_\ell + \mu_\phi)) \frac{1}{k^2 - M_1^2} \hat{\Sigma}_{N_1,R}^{\mathcal{A}}(k) \hat{\Sigma}_{N_1,L}^{\mu\mathcal{A}}(k), \quad (38)$$

¹ In principle, also the first term in the propagator contains an off-shell contribution to the collision term. However, this term is more strongly peaked around the pole than the second one, and it does not depend on the chemical potentials to leading order. We therefore neglect this contribution.

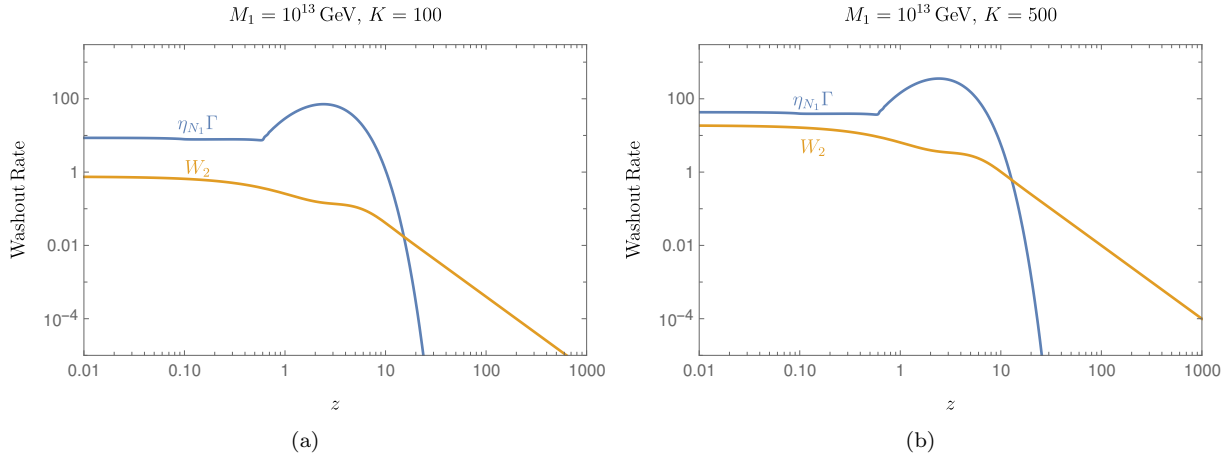


Figure 1. Comparison of washout rates for $\tilde{M}_1 = 10^{13}$ GeV for $K = 100$ (a) and $K = 500$ (b).

which, to first order in the chemical potentials, is

$$g_w \frac{d}{dz} Y_{\ell_{\parallel}} = -\frac{16g_w^2 (h^\dagger h)_{11}^2}{\tilde{M}_1 s} \frac{\mu_\ell + \mu_\phi}{T} \int \frac{d^4 k}{(2\pi)^4} (1 - f_F(k_0)) f_F(k_0) \frac{1}{k^2 - M_1^2} [\hat{\Sigma}_{N_1, R \mu}^{\mathcal{A}}(k) \hat{\Sigma}_{N_1, L}^{\mu \mathcal{A}}(k)]_{\mu_\ell = \mu_\phi = 0}. \quad (39)$$

From this we can extract the new contribution to the washout rate

$$W_2 = -\frac{24K^2}{T^3} \frac{\tilde{M}_1}{T} \left(Y_{\ell_{\parallel}} + \frac{1}{2} Y_\phi \right) \int \frac{d^4 k}{(2\pi)^4} (1 - f_F(k_0)) f_F(k_0) \gamma_{\Delta L=2}(k), \quad (40)$$

with

$$\gamma_{\Delta L=2}(k) = -\frac{(32\pi)^2}{T} \frac{1}{k^2 - M_1^2} \hat{\Sigma}_{N_1 \mu}(k) \hat{\Sigma}_{N_1}^{\mu}(k), \quad (41)$$

which correspond to the $\Delta L = 2$ scattering processes. Note that, since the chemical potentials appear in both $\Sigma_{N_1, L}$ and $\Sigma_{N_1, R}$, when expanding in the chemical potentials we pick up a factor of 2 compared to if we had only considered the potentials from either particles or antiparticles. Since the part of the propagator producing these processes is purely off shell, no real-intermediate-state subtraction is necessary. As expected, these processes do not produce a backreaction into $Y_{N_1 \text{odd}}$ since $\text{tr}[P_h \gamma^5 \gamma^\mu \Sigma_{N_1}^{\mathcal{A}}] \Sigma_{N_1 \mu}^{\mathcal{A}} = 0$.

In Fig. 1, we show the $\Delta L = 2$ rates W_2 compared to the $\Delta L = 1$ rates $\eta_{N_1} \Gamma$. At large z , the rate W_2 scales as z^{-2} , in agreement with Refs. [24, 37], which is a slower suppression than the exponential Boltzmann suppression from $\eta_{N_1} \Gamma$. In this region, after all other processes have frozen out, the $\Delta L = 2$ processes continue to erase the resulting asymmetry. Numerical solutions of the Boltzmann equation with and without these new processes are shown in Fig. 2. In Fig. 3, we present a comparison of the solutions with fully and partially equilibrated spectators in our new analysis including the $\Delta L = 2$ rates. As can be seen from the plots, even with strong washout, the spectator processes substantially change the dynamics of the fields and can lead to differences of several orders of magnitude in the outcomes. In particular, the sign shift that happens at $z \approx 1$ with fully equilibrated spectators is absent once effects from partial equilibration of spectators and thereby the protection of early asymmetries from washout are included.

V. Parameter Scan

We solved the fluid equations numerically from $z = 0.01$ to $z = 1000$ for both vanishing and thermal initial conditions, varying K between 10^{-2} and 10^3 and M_1 between 10^{10} GeV and 10^{16} GeV, and compare the scenarios with fully and partially equilibrated spectators. The results are shown in Fig. 4. With fully equilibrated spectators, we find that the previous bound of $m_{\text{lightest}} \lesssim 0.12$ eV gets tightened to 0.08 eV, probably due to the improved treatment of the $\Delta L = 2$ processes leading to a larger rate than used in Ref. [2]. With partially equilibrated spectators, however, we find that the spectators protect part of the

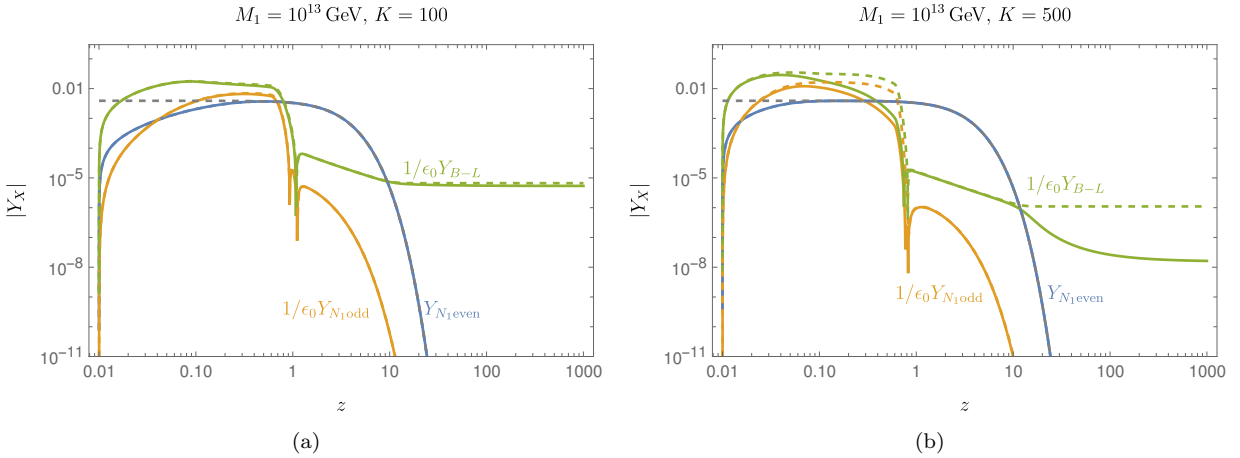


Figure 2. Numerical solutions of Boltzmann equations with fully equilibrated spectators with (solid lines) and without (dashed lines) $\Delta L = 2$ processes for $\tilde{M}_1 = 10^{13}$ GeV for $K = 100$ (a) and $K = 500$ (b).

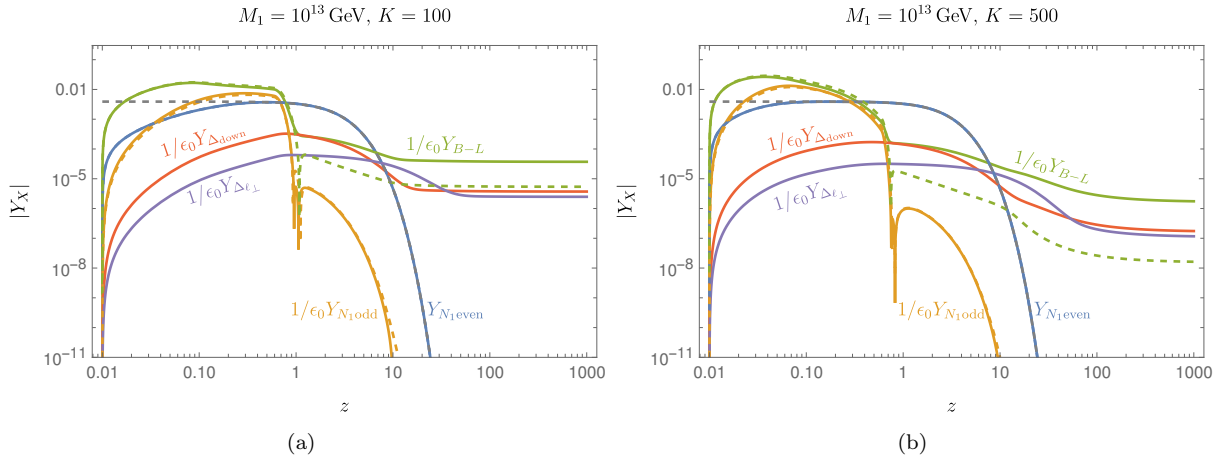


Figure 3. Numerical solutions of Boltzmann equations with partially (solid lines) and fully equilibrated (dashed lines) spectators for $\tilde{M}_1 = 10^{13}$ GeV for $K = 100$ (a) and $K = 500$ (b).

asymmetry from washout. This effect antagonizes the larger $\Delta L = 2$ washout rates. Taking all this into account, sufficient asymmetries for m_{lightest} as large as 0.15 eV can result. We further find a lower bound on M_1 of 10^{10} GeV, which is slightly stronger than the Davidson-Ibarra bound [42].

The impact of increasing the active neutrino masses is twofold. On the one hand, we have the constraint $K \propto \tilde{m}_1 \geq m_{\text{lightest}}$, which implies that increasing neutrino masses restricts K to larger values, where washout is increasingly efficient. On the other hand, as discussed in Refs. [2, 20], increasing the neutrino masses also limits the asymmetry parameter. While one could circumvent this by increasing M_1 , this would simultaneously increase the $\Delta L = 2$ washout rate, as pointed out in Refs. [2, 24, 37], thereby also reducing the final asymmetry. With this, we do not find any allowed region for $m_{\text{lightest}} \geq 0.15$ eV, which gives us an upper bound $m_{\text{lightest}} \lesssim 0.15$ eV for leptogenesis in this scenario.

The plots in Fig. 4 are produced assuming normal hierarchy, but the difference to inverted hierarchy is negligible. The only term which is sensitive to the hierarchy is the maximal decay asymmetry. However, Eq. (4) is valid for both hierarchies, and the main difference between them is that m_1 and m_3 exchange roles as m_{lightest} . Doing the substitution $m_1 \leftrightarrow m_3$ leads to a relative minus sign in Eq. (4), which can be compensated by a change in the sign of y . Therefore, the only practical difference between the two hierarchies is in the precise value of the absolute mass splitting between m_1 and m_3 , which is negligible for our purposes.

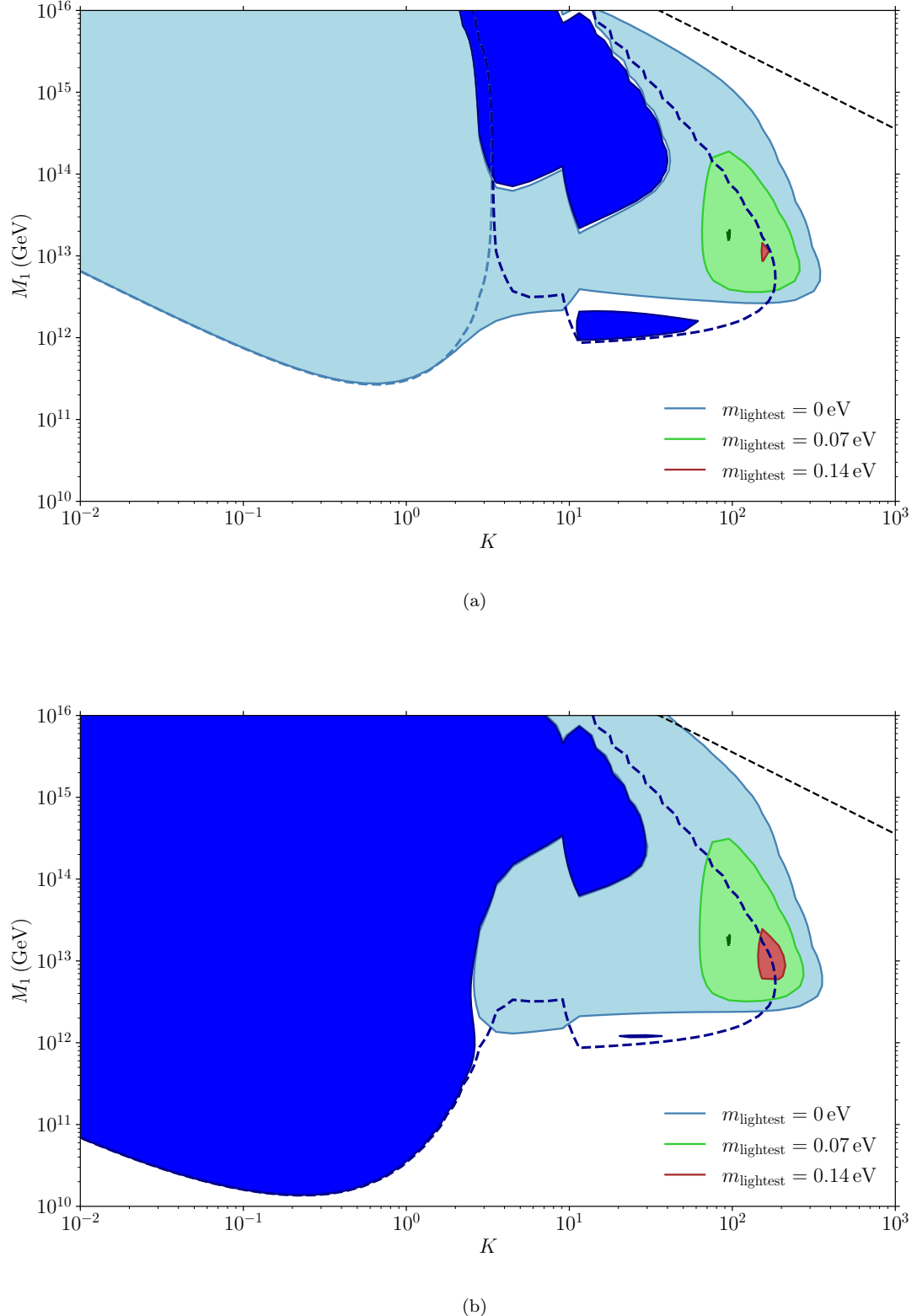


Figure 4. Allowed regions for vanishing (a) and thermal (b) initial conditions and different choices of m_{lightest} . Lighter/darker shades represent different signs of the final asymmetry. The shaded regions are with partially equilibrated spectators, while the dashed contours are with fully equilibrated spectators.

VI. Conclusions

In this work we have applied state-of-the-art techniques to unflavoured leptogenesis in a type-I seesaw model with hierarchical right-handed neutrinos. For this, we have derived $\Delta L = 2$ washout processes within the CTP-formalism and included them in our analysis, thus generalizing the computation from Ref. [14]. We then used these methods to perform a parametric survey of a specific part of the parameter space for leptogenesis in the type-I seesaw mechanism. In particular we revisited the neutrino mass bound from Refs. [1–3]. The spectator fields significantly alter the evolution of the fields, leading to a relative sign change with respect to the scenario without spectators in large regions of the parameter space. They also protect the asymmetry from washout, leading to freeze-out asymmetries which are up to a few orders of magnitude larger than without them. With this, we obtain that the previously reported upper bound on the active neutrino masses for leptogenesis in this scenario is slightly relaxed, even though we use larger $\Delta L = 2$ rates. While the change in the bound appears marginal because of the competing effects, the picture of the underlying dynamics is substantially altered by our use of the up-to-date methods.

As one reduces the mass of N_1 , different spectator processes come into play, as well as flavour effects on the charged leptons. The same methods presented in this work could be applied to these scenarios, potentially leading to a significant change in the outcome of leptogenesis. In general, however, we expect spectator effects, in particular the interplay of their partial equilibration with early asymmetries, to enhance the freeze-out asymmetries, thus opening up viable parameter space for leptogenesis.

Acknowledgements

We would like to thank Carlos Tamarit for very useful discussions and for sharing the code as well as the numerical results from Ref. [14]. E.W.’s work is funded by the Deutsche Forschungsgemeinschaft (DFG, German Research Foundation) – SFB 1258 – 283604770.

A. Review of the CTP formalism

The principal idea of the CTP formalism is to perform a functional integration on a closed time contour, allowing one to compute and track expectation values of operators over time. With this we can, for instance, compute the evolution of particle number densities in the early Universe [33]. As for the usual path-integral, we can compute n -point functions from the CTP path-integral, except that we now must distinguish between the branches going forward (“+”) and backward in time (“-”). The four CTP propagators for a complex scalar field ϕ are then [26, 43–45]

$$i\Delta_X^{++}(u, v) = \langle T\phi_X(u)\phi_X^\dagger(v) \rangle, \quad i\Delta_X^{--}(u, v) = \langle \bar{T}\phi_X(u)\phi_X^\dagger(v) \rangle, \quad (\text{A1a})$$

$$i\Delta_X^<(u, v) = \langle \phi_X^\dagger(v)\phi_X(u) \rangle, \quad i\Delta_X^>(u, v) = \langle \phi_X(u)\phi_X^\dagger(v) \rangle, \quad (\text{A1b})$$

while for a fermion field ψ we have, similarly,

$$iS_{X,\alpha,\beta}^{++}(u, v) = \langle T\psi_{X,\alpha}(u)\bar{\psi}_{X,\beta}(v) \rangle, \quad iS_{X,\alpha,\beta}^{--}(u, v) = \langle \bar{T}\psi_{X,\alpha}(u)\bar{\psi}_{X,\beta}(v) \rangle, \quad (\text{A2a})$$

$$iS_{X,\alpha,\beta}^<(u, v) = -\langle \bar{\psi}_{X,\beta}(v)\psi_{X,\alpha}(u) \rangle, \quad iS_{X,\alpha,\beta}^>(u, v) = \langle \psi_{X,\alpha}(u)\bar{\psi}_{X,\beta}(v) \rangle. \quad (\text{A2b})$$

For an arbitrary two-point function G^{ab} we define retarded and advanced two-point functions

$$G^a = G^T - G^> = G^< - G^{\bar{T}} \quad G^r = G^T - G^< = G^> - G^{\bar{T}} \quad (\text{A3a})$$

as well as spectral and Hermitian functions

$$G^{\mathcal{A}} = \frac{1}{2i}(G^a - G^r) = \frac{i}{2}(G^> - G^<) \quad G^{\mathcal{H}} = \frac{1}{2}(G^a + G^r) = \frac{1}{2}(G^T - G^{\bar{T}}). \quad (\text{A3b})$$

It is further useful to work in Wigner space, where the Wigner transform of a two-point function is defined as

$$G(x, k) = \int d^4r e^{ikr} G\left(x + \frac{r}{2}, x - \frac{r}{2}\right), \quad (\text{A4})$$

which depends both on the momentum k and on the center of mass coordinate x . The two-point functions satisfy Schwinger-Dyson equations [33, 46], which, in Wigner space, are given by [43]

$$e^{-i\diamond}\{k^2 - m_X^2 - \Pi_X^{a,r}\}\{\Delta_X^{a,r}\} = 1, \quad (\text{A5a})$$

$$e^{-i\diamond}\{k^2 - m_X^2 - \Pi_X^r\}\{\Delta_X^{<,>}\} = e^{-i\diamond}\{\Pi_X^{<,>}\}\{\Delta_X^a\}, \quad (\text{A5b})$$

$$e^{-i\diamond}\{\not{k} - m_X - \Sigma_X^{a,r}\}\{iS_X^{a,r}\} = iP_X, \quad (\text{A5c})$$

$$e^{-i\diamond}\{\not{k} - m_X - \Sigma_X^r\}\{iS_X^{<,>}\} = e^{-i\diamond}\{\Sigma_X^{<,>}\}\{iS_X^a\}, \quad (\text{A5d})$$

with the diamond operator \diamond defined as

$$\diamond\{A(x, k)\}\{B(x, k)\} = \frac{1}{2}[(\partial_x^\mu A(x, k))(\partial_{k,\mu}B(x, k)) - (\partial_k^\mu A(x, k))(\partial_{x,\mu}B(x, k))], \quad (\text{A6})$$

and the scalar and fermionic self-energies

$$\Pi_X^{ab}(u, v) = iab \frac{\delta\Gamma^{2\text{PI}}}{\delta\Delta^{ba}(v, u)}, \quad (\text{A7a})$$

$$\Sigma_X^{ab}(u, v) = -iab \frac{\delta\Gamma^{2\text{PI}}}{\delta S_X^{ba}(v, u)}, \quad (\text{A7b})$$

where the functional $\Gamma^{2\text{PI}}$ is minus i times the sum of the two-particle irreducible vacuum graphs.

To zeroth order in the gradients and to leading order in the Yukawa couplings, the Schwinger-Dyson equations are

$$(k^2 - m_X^2 - \Pi_X^{a,r})\Delta_X^{a,r} = 1, \quad (\text{A8a})$$

$$(k^2 - m_X^2 - \Pi_X^r)\Delta_X^{<,>} = \Pi_X^{<,>}\Delta_X^a, \quad (\text{A8b})$$

$$(\not{k} - m_X - \Sigma_X^{a,r})iS_X^{a,r} = iP_X, \quad (\text{A8c})$$

$$(\not{k} - m_X - \Sigma_X^r)iS_X^{<,>} = \Sigma_X^{<,>}iS_X^a. \quad (\text{A8d})$$

In kinetic equilibrium, Eqs. (A8b) and (A8d) give

$$i\Delta_X^{<}(k) = 2\Delta_X^A f_X(k), \quad i\Delta_X^{>}(k) = 2\Delta_X^A(1 + f_X(k)), \quad (\text{A9a})$$

$$iS_X^{<}(k) = -2S_X^A(k)f_X(k), \quad iS_X^{>}(k) = 2S_X^A(k)(1 - f_X(k)), \quad (\text{A9b})$$

where $f_X(k)$ are equilibrium distributions with chemical potential μ_X :

$$f_X(k) = \frac{1}{e^{\beta(k_0 - \mu_X)} + 1} \text{ (fermions)}, \quad f_X(k) = \frac{1}{e^{\beta(k_0 - \mu_X)} - 1} \text{ (bosons)}. \quad (\text{A10})$$

The spectral functions can be obtained from Eqs. (A8a) and (A8c). At tree level, they are given by

$$\Delta_X^{A,\text{tree}}(k) = \pi\delta(k^2 - m_X^2)\text{sign}(k_0), \quad (\text{A11a})$$

$$S_X^{A,\text{tree}}(k) = \pi\delta(k^2 - m_X^2)\text{sign}(k_0)P_X(\not{k} + m_X), \quad (\text{A11b})$$

while the spectral functions with the loop insertions summed up are given by

$$S_X^A(k) = P_X \left[(\not{k} + m_X - \Sigma_X^H(k)) \cdot \frac{\Gamma_X}{\Omega_X^2 + \Gamma_X^2} - \Sigma_X^A(k) \frac{\Omega_X}{\Omega_X^2 + \Gamma_X^2} \right], \quad \Delta_X^A(k) = \frac{\Gamma_X}{\Omega_X^2 + \Gamma_X^2}, \quad (\text{A12})$$

with

$$\Gamma_X(k) = 2(k_\mu - \Sigma_{X,\mu}^H) \cdot \Sigma_X^{A,\mu}, \quad \Omega_X(k) = (k_\mu - \Sigma_{X,\mu}^H)^2 - m_X^2 - (\Sigma_{X,\mu}^A)^2, \quad (\text{A13})$$

for fermions and

$$\Gamma_X(k) = \Pi_X^A, \quad \Omega_X(k) = k^2 - m_X^2 - \Pi_X^H, \quad (\text{A14})$$

for scalars.

A short comment on the derivation of Eq. (38) is in order here. In order to go from Eq. (36) to Eq. (38), we made use of the KMS relation

$$\hat{\Sigma}_{N_1,L/R}^>(k) = -e^{(k_0 \mp \mu_\ell \mp \mu_\phi)/T} \hat{\Sigma}_{N_1,L/R}^<(k), \quad (\text{A15})$$

which, inserted into Eq. (A8b), implies

$$S_{N_1,L/R}^>(k) = -e^{(k_0 \mp \mu_\ell \mp \mu_\phi)/T} S_{N_1,L/R}^<(k). \quad (\text{A16})$$

Taken at face value, this would mean that N_1 , ℓ and ϕ are in chemical equilibrium, with $\mu_{N_1,L/R} = \pm \mu_\ell \pm \mu_\phi$, which would indeed be the case if ℓ and ϕ were in chemical equilibrium with N_1 . As it turns out, however, N_1 is not in chemical equilibrium, and its out-of-equilibrium decays drive ℓ and ϕ out of equilibrium. The use of equilibrium distribution functions for ℓ and ϕ here is merely an approximation in order to obtain the off-shell piece of the propagator for N_1 . We therefore emphasize that applying the KMS relation Eq. (A16) to the on-shell part of the propagator does not make sense. However, concerning the off-shell part of the propagator, we can interpret this relation to apply to Σ_{N_1} and to the fields therein, and not to N_1 explicitly. Since we do approximate the fields contained in Σ_{N_1} as being in kinetic equilibrium, it does make sense to use Eq. (A16) for this off-shell part. This is the origin of the additional factor of two, which is characteristic of $\Delta L = 2$ processes.

[1] W. Buchmuller, P. Di Bari, and M. Plumacher, A Bound on neutrino masses from baryogenesis, *Phys. Lett. B* **547**, 128 (2002), arXiv:hep-ph/0209301.

[2] W. Buchmuller, P. Di Bari, and M. Plumacher, The Neutrino mass window for baryogenesis, *Nucl. Phys. B* **665**, 445 (2003), arXiv:hep-ph/0302092.

[3] G. F. Giudice, A. Notari, M. Raidal, A. Riotto, and A. Strumia, Towards a complete theory of thermal leptogenesis in the SM and MSSM, *Nucl. Phys. B* **685**, 89 (2004), arXiv:hep-ph/0310123.

[4] N. Aghanim *et al.* (Planck), Planck 2018 results. VI. Cosmological parameters, *Astron. Astrophys.* **641**, A6 (2020), [Erratum: *Astron. Astrophys.* 652, C4 (2021)], arXiv:1807.06209 [astro-ph.CO].

[5] A. G. Adame *et al.* (DESI), DESI 2024 VI: Cosmological Constraints from the Measurements of Baryon Acoustic Oscillations (2024), arXiv:2404.03002 [astro-ph.CO].

[6] E. Di Valentino and A. Melchiorri, Neutrino Mass Bounds in the Era of Tension Cosmology, *Astrophys. J. Lett.* **931**, L18 (2022), arXiv:2112.02993 [astro-ph.CO].

[7] S. Gariazzo, O. Mena, and T. Schwetz, Quantifying the tension between cosmological and terrestrial constraints on neutrino masses, *Phys. Dark Univ.* **40**, 101226 (2023), arXiv:2302.14159 [hep-ph].

[8] T. Sekiguchi and T. Takahashi, Cosmological bound on neutrino masses in the light of H_0 tension, *Phys. Rev. D* **103**, 083516 (2021), arXiv:2011.14481 [astro-ph.CO].

[9] M. Forconi, E. Di Valentino, A. Melchiorri, and S. Pan, Possible impact of non-Gaussianities on cosmological constraints in neutrino physics, *Phys. Rev. D* **109**, 123532 (2024), arXiv:2311.04038 [astro-ph.CO].

[10] J.-Q. Jiang, W. Giarè, S. Gariazzo, M. G. Dainotti, E. Di Valentino, O. Mena, D. Pedrotti, S. S. da Costa, and S. Vagnozzi, Neutrino cosmology after DESI: tightest mass upper limits, preference for the normal ordering, and tension with terrestrial observations (2024), arXiv:2407.18047 [astro-ph.CO].

[11] M. Aker *et al.* (KATRIN), Direct neutrino-mass measurement with sub-electronvolt sensitivity, *Nature Phys.* **18**, 160 (2022), arXiv:2105.08533 [hep-ex].

[12] A. Gando *et al.* (KamLAND-Zen), Search for Majorana Neutrinos near the Inverted Mass Hierarchy Region with KamLAND-Zen, *Phys. Rev. Lett.* **117**, 082503 (2016), [Addendum: *Phys. Rev. Lett.* 117, 109903 (2016)], arXiv:1605.02889 [hep-ex].

[13] S. Abe *et al.* (KamLAND-Zen), Search for the Majorana Nature of Neutrinos in the Inverted Mass Ordering Region with KamLAND-Zen, *Phys. Rev. Lett.* **130**, 051801 (2023), arXiv:2203.02139 [hep-ex].

[14] B. Garbrecht, P. Klose, and C. Tamarit, Relativistic and spectator effects in leptogenesis with heavy sterile neutrinos, *JHEP* **02**, 117, arXiv:1904.09956 [hep-ph].

[15] S. Blanchet and P. Di Bari, The minimal scenario of leptogenesis, *New J. Phys.* **14**, 125012 (2012), arXiv:1211.0512 [hep-ph].

[16] P. Di Bari, Seesaw geometry and leptogenesis, *Nucl. Phys. B* **727**, 318 (2005), arXiv:hep-ph/0502082.

[17] M. Flanz, E. A. Paschos, and U. Sarkar, Baryogenesis from a lepton asymmetric universe, *Phys. Lett. B* **345**, 248 (1995), [Erratum: *Phys. Lett. B* 384, 487–487 (1996), Erratum: *Phys. Lett. B* 382, 447–447 (1996)], arXiv:hep-ph/9411366.

[18] L. Covi, E. Roulet, and F. Vissani, CP violating decays in leptogenesis scenarios, *Phys. Lett. B* **384**, 169 (1996), arXiv:hep-ph/9605319.

[19] W. Buchmuller and M. Plumacher, CP asymmetry in Majorana neutrino decays, *Phys. Lett. B* **431**, 354 (1998), arXiv:hep-ph/9710460.

[20] T. Hambye, Y. Lin, A. Notari, M. Papucci, and A. Strumia, Constraints on neutrino masses from leptogenesis models, *Nucl. Phys. B* **695**, 169 (2004), arXiv:hep-ph/0312203.

[21] J. N. Fry, K. A. Olive, and M. S. Turner, Hierarchy of Cosmological Baryon Generation, *Phys. Rev. Lett.* **45**, 2074 (1980).

[22] M. Fukugita and T. Yanagida, Baryogenesis Without Grand Unification, *Phys. Lett. B* **174**, 45 (1986).

[23] M. Plumacher, Baryogenesis and lepton number violation, *Z. Phys. C* **74**, 549 (1997), arXiv:hep-ph/9604229.

[24] W. Buchmuller, P. Di Bari, and M. Plumacher, Leptogenesis for pedestrians, *Annals Phys.* **315**, 305 (2005), arXiv:hep-ph/0401240.

[25] R. Barbieri, P. Creminelli, A. Strumia, and N. Tetradis, Baryogenesis through leptogenesis, *Nucl. Phys. B* **575**, 61 (2000), arXiv:hep-ph/9911315.

[26] M. Beneke, B. Garbrecht, M. Herranen, and P. Schwaller, Finite Number Density Corrections to Leptogenesis, *Nucl. Phys. B* **838**, 1 (2010), arXiv:1002.1326 [hep-ph].

[27] J. Ghiglieri and M. Laine, GeV-scale hot sterile neutrino oscillations: a numerical solution, *JHEP* **02**, 078, arXiv:1711.08469 [hep-ph].

[28] T. Asaka, S. Ejima, and H. Ishida, Kinetic Equations for Baryogenesis via Sterile Neutrino Oscillation, *JCAP* **02**, 021, arXiv:1112.5565 [hep-ph].

[29] A. Basboll and S. Hannestad, Decay of heavy Majorana neutrinos using the full Boltzmann equation including its implications for leptogenesis, *JCAP* **01**, 003, arXiv:hep-ph/0609025.

[30] F. Hahn-Woernle, M. Plumacher, and Y. Y. Y. Wong, Full Boltzmann equations for leptogenesis including scattering, *JCAP* **08**, 028, arXiv:0907.0205 [hep-ph].

[31] J. S. Schwinger, Brownian motion of a quantum oscillator, *J. Math. Phys.* **2**, 407 (1961).

[32] L. V. Keldysh, Diagram technique for nonequilibrium processes, *Zh. Eksp. Teor. Fiz.* **47**, 1515 (1964).

[33] E. Calzetta and B. L. Hu, Nonequilibrium Quantum Fields: Closed Time Path Effective Action, Wigner Function and Boltzmann Equation, *Phys. Rev. D* **37**, 2878 (1988).

[34] B. Garbrecht and P. Schwaller, Spectator Effects during Leptogenesis in the Strong Washout Regime, *JCAP* **10**, 012, arXiv:1404.2915 [hep-ph].

[35] B. Garbrecht, F. Głowna, and P. Schwaller, Scattering Rates For Leptogenesis: Damping of Lepton Flavour Coherence and Production of Singlet Neutrinos, *Nucl. Phys. B* **877**, 1 (2013), arXiv:1303.5498 [hep-ph].

[36] G. D. Moore, Do we understand the sphaleron rate?, in *4th International Conference on Strong and Electroweak Matter* (2000) pp. 82–94, arXiv:hep-ph/0009161.

[37] W. Buchmuller, P. Di Bari, and M. Plumacher, Cosmic microwave background, matter - antimatter asymmetry and neutrino masses, *Nucl. Phys. B* **643**, 367 (2002), [Erratum: *Nucl.Phys.B* 793, 362 (2008)], arXiv:hep-ph/0205349.

[38] E. W. Kolb and S. Wolfram, Baryon Number Generation in the Early Universe, *Nucl. Phys. B* **172**, 224 (1980), [Erratum: *Nucl.Phys.B* 195, 542 (1982)].

[39] B. Garbrecht and M. Garny, Finite Width in out-of-Equilibrium Propagators and Kinetic Theory, *Annals Phys.* **327**, 914 (2012), arXiv:1108.3688 [hep-ph].

[40] F. Głowna, *Right-handed Neutrino Production at Finite Temperatures: Radiative Corrections, Soft and Collinear Divergences*, Ph.D. thesis, Munich, Tech. U. (2015).

[41] B. Garbrecht, F. Głowna, and M. Herranen, Right-Handed Neutrino Production at Finite Temperature: Radiative Corrections, Soft and Collinear Divergences, *JHEP* **04**, 099, arXiv:1302.0743 [hep-ph].

[42] S. Davidson and A. Ibarra, A Lower bound on the right-handed neutrino mass from leptogenesis, *Phys. Lett. B* **535**, 25 (2002), arXiv:hep-ph/0202239.

[43] T. Prokopec, M. G. Schmidt, and S. Weinstock, Transport equations for chiral fermions to order h bar and electroweak baryogenesis. Part 1, *Annals Phys.* **314**, 208 (2004), arXiv:hep-ph/0312110.

[44] B. Garbrecht, Why is there more matter than antimatter? Calculational methods for leptogenesis and electroweak baryogenesis, *Prog. Part. Nucl. Phys.* **110**, 103727 (2020), arXiv:1812.02651 [hep-ph].

[45] M. Beneke, B. Garbrecht, C. Fidler, M. Herranen, and P. Schwaller, Flavoured Leptogenesis in the CTP Formalism, *Nucl. Phys. B* **843**, 177 (2011), arXiv:1007.4783 [hep-ph].

[46] J. M. Cornwall, R. Jackiw, and E. Tomboulis, Effective Action for Composite Operators, *Phys. Rev. D* **10**, 2428 (1974).